ELSEVIER

International Journal of Heat and Fluid Flow 20 (1999) 446–452

International Journal of HEAT AND FLUID FLOW

www.elsevier.com/locate/ijhff

Melting of unfixed solids in square cavities

B. Ghasemi, M. Molki *,1

Department of Mechanical Engineering, Isfahan University of Technology, Isfahan 84154, Iran

Received 27 September 1997; accepted 11 February 1999

Abstract

A fixed-grid enthalpy method is employed to study the melting of an unfixed solid in a square cavity. The cavity is initially filled with the solid material. The walls are heated and the solid is released as a result of melting near the walls. Falling of the solid in the melt and the buoyancy are the main factors affecting the liquid motion and the melting process. The problem is studied numerically and the results are validated by a comparison with the available analytical, numerical, and experimental results. The computations are carried out for the Rayleigh numbers 0–10^8 and the Archimedes numbers 0–10^7. The results are reported for the liquid percent, falling velocity of the solid phase, and shape of the solid–liquid interface. It was found that at low Rayleigh and Archimedes numbers, the melting rate and the solid velocity are both very low, and the melting is almost symmetrical. Higher values of Rayleigh and Archimedes numbers enhance melting and the falling velocity of the solid and distort the symmetry of the interface.

Keywords: Heat transfer; Unfixed solid; Cavity; Melting; Enthalpy method

Notation

A	aspect ratio, W/L
Ar	Archimedes number, $(\rho_s - \rho)gL^3/\rho\nu^2$
c	specific heat, J/kg K
h	sensible enthalpy, J/kg
H	dimensionless sensible enthalpy, $(h - h_m)/c(T_w - T_m)$
k	thermal conductivity, W/m K
L	horizontal dimension of the cavity, m
p	pressure
p'	modified pressure, $p + \rho_m gy$
P	dimensionless pressure, $p'L^2/\rho\nu^2$
Pr	Prandtl number, ν/α
q	heat transfer rate
q^*	dimensionless heat transfer
Q	total heat for complete melting of the solid
Ra	Rayleigh number, $g\beta L^3(T_w - T_m)/\nu\alpha$
S	source term
St	Stefan number, $c(T_w - T_m)/\lambda$
t	time
T	temperature
u	x-component of velocity
U	dimensionless x-component of velocity, uL/ν
v	y-component of velocity
V	dimensionless y-component of velocity, vL/ν
W	height of the enclosure, m
x	horizontal coordinate
X	dimensionless horizontal coordinate, x/L
y	vertical coordinate
Y	dimensionless vertical coordinate, y/L

Greek

α	thermal diffusivity, m^2/s
β	volumetric thermal expansion coefficient, 1/K
ΔH	nodal latent heat, J/kg
$\Delta\tau$	dimensionless time step
ΔV	solid volume
ε	solid fraction, $1 - \Delta H/\lambda$
ϕ	subcooling parameter, $(T_m - T_i)/(T_w - T_m)$
λ	latent heat of fusion, J/kg
μ	dynamic viscosity, kg/m s
ρ	density, kg/m^3
τ	dimensionless time, vt/L^2
ν	kinematic viscosity, m^2/s

Subscripts

h	refers to energy equation
H	refers to dimensionless energy equation
i	initial value
l	liquid phase
m	melting point
n	iteration counter
P	identifies node P
s	solid phase
t	refers to top solid surface
u	refers to momentum equation in x direction
U	refers to dimensionless momentum equation in x direction
v	refers to momentum equation in y direction

* Corresponding author. E-mail: molki@eng.umd.edu

[1] Present address: Department of Mechanical Engineering, University of Maryland, College Park, MD 20742, USA.

0142-727X/99/$ – see front matter
PII: S0142-727X(99)00025-9

V refers to dimensionless momentum equation in y direction
w refers to wall

1. Introduction

There are numerous engineering applications where phase-change phenomena are present. These include casting, welding, molding, crystal growth, storage and transport of thermal energy, and so on. Therefore, significant efforts have been devoted to modeling these moving-boundary problems (Crank, 1984).

In early work in this area, conduction was assumed to be the main mode of heat transfer. The problems of this type, therefore, could be solved by analytical methods (Zerrokal and Chatwin, 1994). In more practical problems, however, natural convection in the melt plays an important role on the shape and motion of the solid–liquid interface. This effect has been well investigated in the past by the experimental and numerical methods (Gau and Viskanta, 1986; Beeckermann and Viskanta, 1989; Rady and Mohanty, 1996; Chang and Yang, 1996).

The density difference between the liquid and solid phases is another important factor in phase-change problems. If melting takes place in a rectangular cavity with all walls heated, the heavy solid phase moves downward due to gravity against the bottom wall. In this situation, the significant part of melting takes place in the narrow contact area between the moving solid and the stationary bottom wall. This type of melting, known as contact melting, has been treated experimentally (Bareiss and Beer, 1984; Moallemi et al., 1986; Dong et al., 1991), analytically (Moallemi and Viskanta, 1986; Roy and Sengupta, 1990), and numerically (Yoo and Ro, 1988).

In the analysis of contact melting problems, it is generally assumed that the liquid film under the solid is thin and the inertia terms in the governing equations are neglected. These assumptions are only valid when the solid phase is much denser than the liquid or when the solid is pressed against the hot wall by force. In low gravity environments, or when the solid is just slightly denser than the liquid, the melting zone is large with considerable fluid motion and interface deformation. This is a more practical situation in many engineering problems, and it can not be analyzed by the thin-film assumption of the contact melting.

The objective of the present paper is to numerically solve the melting of unfixed solid phase in a rectangular cavity without any assumption regarding the melting region. The conservation equations are applied to the whole solution domain comprising the solid and liquid phases. The latent heat of fusion is accounted for by including a suitable source term in the energy equation. To establish a constant velocity in the moving solid phase, either a source term is added to the momentum equations (Voller and Prakash, 1987; Brent and Voller, 1988) or viscosity functions are employed to generate the liquid viscosity in the liquid and a large viscosity in the solid (Prakash et al., 1987; Benon and Incropera, 1988; Cao and Faghri, 1990). In the present study, the viscosity function approach was employed.

The search of the literature revealed that the work of Asako et al. (1994) is the most related investigation to the present work. There are, however, several new features in the present study that are not treated there: The buoyancy-induced motion in the liquid in addition to the motion caused by falling solid, all the cavity walls are heated simultaneously and the solid is melting from all sides and not just from below, melting is continued until the complete melting of the solid phase, and the complete geometrical history of the solid–liquid interface.

2. Mathematical formulation

The simplified view of the cavity is shown in Fig. 1. Initially, the cavity is filled with the solid at uniform temperature $T_i - T_m$. At time $t = 0$, the temperature of all walls are suddenly raised to $T_w > T_m$, with T_m the melting temperature of the solid material. With this arrangement, melting begins all around the solid, and the solid moves downward. Assuming, (1) laminar, incompressible, and 2D convection in the melt, (2) Newtonian fluid, (3) constant properties in all phases, except for the viscosity and the density in buoyancy terms, (4) Boussinesq approximation, and (5) neglecting the solid velocity in the x direction, and considering the solid phase as a liquid with infinite viscosity, the governing differential equations are,

Continuity:

$$\frac{\partial u}{\partial x} + \frac{\partial v}{\partial y} = 0. \tag{1}$$

Momentum:

$$\rho \frac{\partial u}{\partial t} + \rho u \frac{\partial u}{\partial x} + \rho v \frac{\partial u}{\partial y} = -\frac{\partial p}{\partial x} + \mu^* \left(\frac{\partial^2 u}{\partial x^2} + \frac{\partial^2 u}{\partial y^2} \right), \tag{2}$$

$$\rho \frac{\partial v}{\partial t} + \rho u \frac{\partial v}{\partial x} + \rho v \frac{\partial v}{\partial y} = -\frac{\partial p}{\partial y} + \mu^* \left(\frac{\partial^2 v}{\partial x^2} + \frac{\partial^2 v}{\partial y^2} \right) - \rho^* g. \tag{3}$$

Energy:

$$\rho \frac{\partial h}{\partial t} + \rho u \frac{\partial h}{\partial x} + \rho v \frac{\partial h}{\partial y} = \frac{k}{c} \left(\frac{\partial^2 h}{\partial x^2} + \frac{\partial^2 h}{\partial y^2} \right) + S_h, \tag{4}$$

where $\rho^* = \rho_l$ and $\mu^* = \mu_l$ in liquid, $\rho^* = \rho_s$ and $\mu^* = \mu_s = \infty$ in solid, and $\rho_l < \rho^* < \rho_s$ and $\mu_l < \mu^* < \mu_s$ in the melting region.

The form of the enthalpy source term, S_h, is derived from the total enthalpy formulation, which is expanded as the sum of sensible, h, and latent, ΔH, enthalpies (Voller and Prakash, 1987). The resulting source term is,

$$S_h = -\left(\rho \frac{\partial \Delta H}{\partial t} + \rho u \frac{\partial \Delta H}{\partial x} + \rho v \frac{\partial \Delta H}{\partial y} \right). \tag{5}$$

In isothermal phase change with stationary solid phase, the latent enthalpy is either zero or is equal to the latent heat of fusion, λ, and the last two terms vanish. In the present work, however, the convective terms in Eq. (5) are nonzero due to the motion of the solid phase.

Defining $p' = p + \rho_m g y$, the governing differential equations are rearranged and rewritten in terms of the dimensionless variables as

$$\frac{\partial U}{\partial X} + \frac{\partial V}{\partial Y} = 0, \tag{6}$$

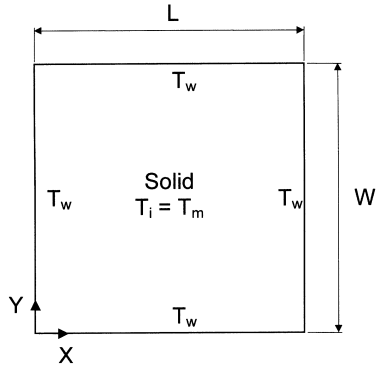

Fig. 1. Schematic view of the square cavity.

$$\frac{\partial U}{\partial \tau}+U\frac{\partial U}{\partial X}+V\frac{\partial U}{\partial Y}=-\frac{\partial P}{\partial X}+f_\mu\left(\frac{\partial^2 U}{\partial X^2}+\frac{\partial^2 U}{\partial Y^2}\right), \tag{7}$$

$$\frac{\partial V}{\partial \tau}+U\frac{\partial V}{\partial X}+V\frac{\partial V}{\partial Y} =-\frac{\partial P}{\partial Y}+f_\mu\left(\frac{\partial^2 V}{\partial X^2}+\frac{\partial^2 V}{\partial Y^2}\right)+\frac{\mathrm{Ra}}{\mathrm{Pr}}H-\varepsilon \mathrm{Ar}, \tag{8}$$

$$\frac{\partial H}{\partial \tau}+U\frac{\partial H}{\partial X}+V\frac{\partial H}{\partial Y}=\frac{1}{\mathrm{Pr}}\left(\frac{\partial^2 H}{\partial X^2}+\frac{\partial^2 H}{\partial Y^2}\right)+S_H, \tag{9}$$

$$S_H=\frac{1}{\mathrm{St}}\left(\frac{\partial \varepsilon}{\partial \tau}+U\frac{\partial \varepsilon}{\partial X}+V\frac{\partial \varepsilon}{\partial Y}\right), \tag{10}$$

where f_μ is the viscosity function and must be 1 in the liquid phase, a large value in the solid phase, and increase gradually from 1 to a large value with the solid fraction, ε. In this study, f_μ was assumed to depend on ε as $f_\mu=10^{5\varepsilon}$.

Although f_μ can be expressed by other functional forms, the abovementioned choice had the merit of good numerical convergence. As the computational mesh is refined, the sensitivity of the results on the choice of viscosity function decreases.

3. The numerical method

The governing differential equations were solved numerically by the control-volume based finite-difference method and the SIMPLE algorithm. The formulation was fully implicit in time and the convection–diffusion terms were treated by the power-law scheme (Patankar, 1980).

The present numerical approach solved the conservation differential equations without considering a separate equation for the motion of solid phase. Asako et al. (1994) employed an additional equation of motion for the solid phase to increase convergence. With the new viscosity function employed in the present work, the computations converged reasonably well.

In each iteration, the solid–liquid interface had to be determined. This could be done by the FLAIR method (Ashgriz and Poo, 1991). FLAIR, however, needed more CPU time, and it could not be used in two-phase problems involving mushy zones, as is the case with alloys. In the present work, the solid–liquid interface was determined based on the value of the liquid fraction.

To evaluate the source term, S_H, in the energy equation, the solid fraction, ε_P, for node P should be iteratively computed as $1-\Delta H_P/\lambda$. Thus, the latent enthalpy for the node, ΔH_P, is required in each iteration. Voller and Prakash (1987) have proposed an effective algorithm for updating the latent heat,

$$\Delta H_{P,n+1}=\Delta H_{P,n}+h_{P,n}-cF^{-1}(\Delta H_{P,n}), \tag{11}$$

where F^{-1} is the inverse of the latent heat function. For the general case of nonpure metals, numerous functional forms of F have been suggested by Chi-Keung Chiu and Caldwell (1996). In this work,

$$\Delta H=F(T)=\begin{cases}0 & T<T_{\mathrm{m}},\\ \lambda & T>T_{\mathrm{m}}\end{cases} \tag{12}$$

The abovementioned numerical method was implemented in a FORTRAN program. Before the onset of the final runs, a number of numerical experiments were carried out for melting of gallium with $\mathrm{Ra}=2.5\times10^6$, $\mathrm{Ar}=3.6\times10^7$, $\mathrm{Pr}=2.16\times10^{-2}$, $\mathrm{St}=4.12\times10^{-2}$, and $\phi=0.171$ in order to validate the program. The effects of grid density and time step are shown in Figs. 2–4. The ordinate V_s in Figs. 2 and 4 is the velocity of the falling solid phase (the positive direction is upward). Based on these results, a 20×40 uniform square grid for half the cavity and a time step of 10^{-5} was employed for the final computations. The convergence criteria were to reduce the maximum mass residual of the grid control volumes below 10^{-5}, and the local relative change in enthalpies to less than 10^{-6}.

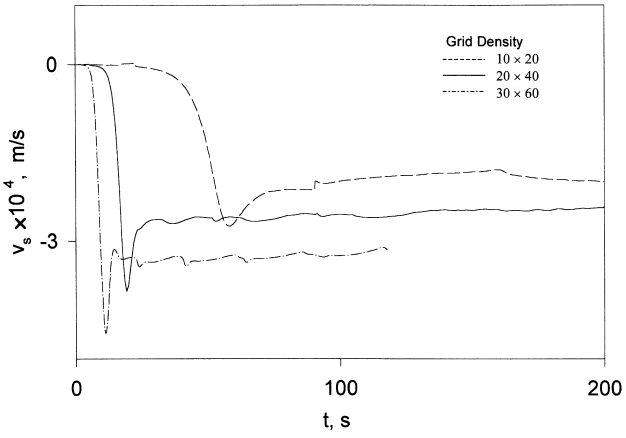

Fig. 2. Effect of grid density on velocity of the solid phase.

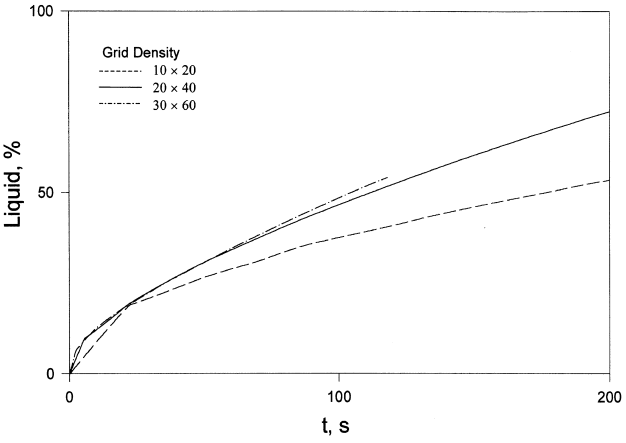

Fig. 3. Effect of grid density on liquid formation.

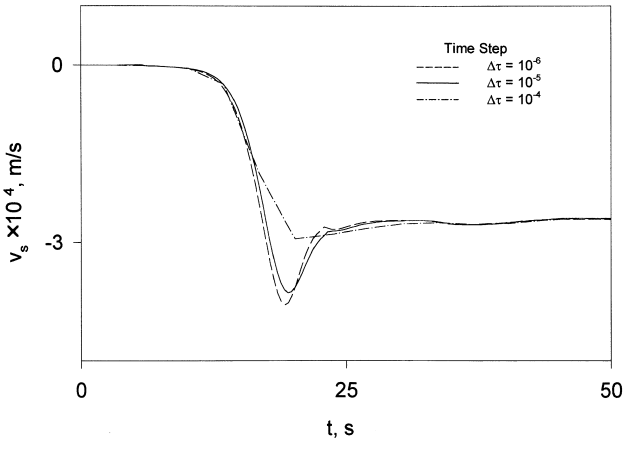

Fig. 4. Effect of time step on velocity of the solid phase.

4. Results and discussion

As a first step, the code was validated by comparing the results for a simple natural convection problem with a well-known benchmark solution. Table 1 compares the natural convection in a rectangular cavity with the benchmark solution of De Vahl Davis (1983). The parameters chosen for comparison are Nusselt number on the wall, Nu_0, Nusselt number on the vertical mid-plane, $Nu_{1/2}$, and stream function on the mid point of the cavity, ψ_{mid}. Richardson extrapolation is used to estimate the order of errors. The method is second order and is in good agreement with the benchmark solution.

Before discussing the melting process with the falling solid phase, comparisons are made between the results obtained by the present method for the fixed-solid melting and the related 1D analytical, 2D numerical and experimental results available in the literature. Table 2 compares the melt thickness of gallium in a 1D conduction melting obtained from the present method with the analytical solution for different grid densities at different times. The numbers in parentheses indicate the differences in percent. It is evident from the table that, as the mesh size is refined, the numerical results approach the analytical solution.

Further comparison is made in Fig. 5 where the interface location for the convection–diffusion melting of gallium in a rectangular enclosure, with the top and bottom walls insulated and other boundary conditions similar to those employed by Gau and Viskanta (1986), and Brent and Voller (1988), is compared. The interface is shown for three different times, namely $t = 3$, 6, and 10 min from the onset of melting. The good agreement between the results is supportive of the present numerical approach.

The last comparison with the literature is given in Fig. 6. In this figure, the solid volume fraction, $\Delta V/\Delta V_i$, and the location of the top solid surface, Y_t, for $Ar = 100$ and $Pr = 10$ are compared with those of Asako et al. (1994). The agreement between Y_t is excellent. The volume fractions, however, are somewhat different at the larger values of time, which is possibly due to the different mesh and time steps.

Attention is now turned to the effect of natural convection on melting with unfixed solid. To eliminate the melt motion induced by the direct falling of the solid phase, Ar is set to

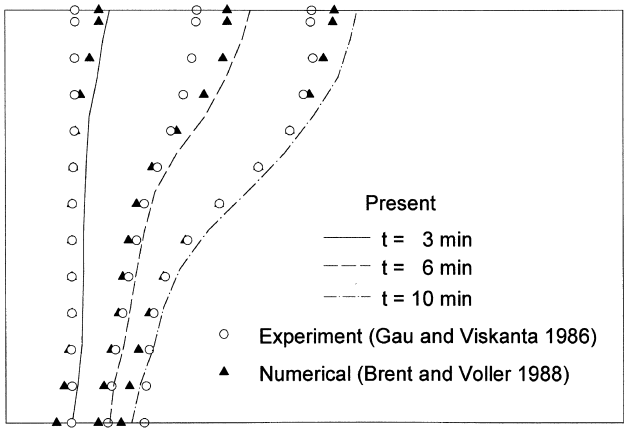

Fig. 5. Comparison with the experimental and numerical results for melting of gallium.

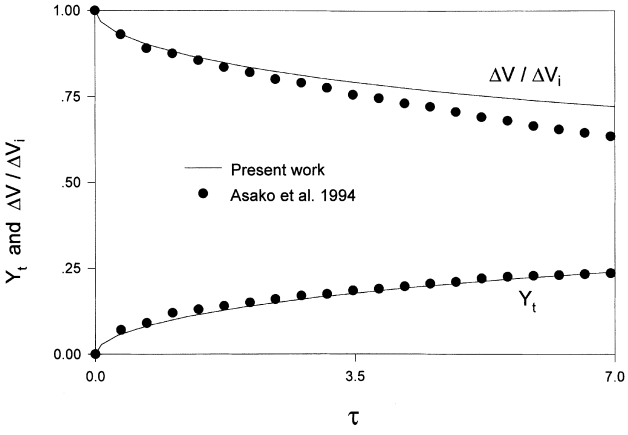

Fig. 6. Comparison with the literature for $Ar = 100$ and $Pr = 10$.

Table 1
Natural convection in a rectangular cavity

	Present work						
	$h = 0.025$	$h = 0.0125$	$h = 0.00625$	Extrapolated	Order of error	De Vahl Davis (1983)	Error (%)
Nu_0	4.619	4.546	4.527	4.520	1.94	4.509	0.24
$Nu_{1/2}$	4.588	4.539	4.526	4.521	1.91	4.519	0.04
ψ_{mid}	13.045	12.891	12.840	12.815	1.61	12.832	−0.13

Table 2
Melt thickness in 1D conduction melting of gallium

Time, min	Grid density				
	0.1	0.05	0.03	0.01	Analytical
10	0.0054	0.012	0.0185	0.0243	0.0248
	(75.2%)	(51.6%)	(25.4%)	(2.0%)	
60	0.0367	0.0578	0.0594	0.0608	0.0609
	(39.7%)	(5.1%)	(2.5%)	(0.2%)	
120	0.0747	0.0828	0.0844	0.0862	0.0861
	(13.2%)	(3.8%)	(2.0%)	(0.1%)	

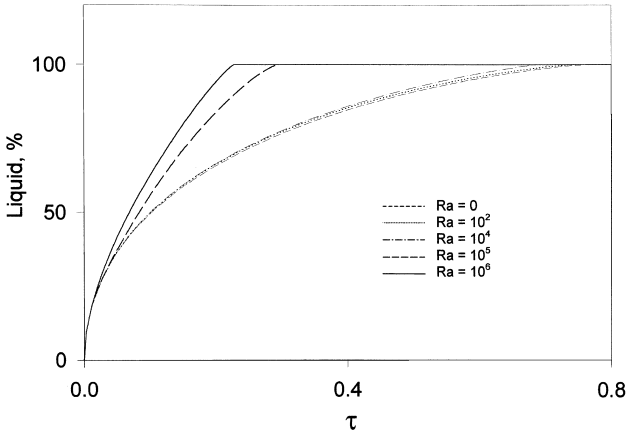

Fig. 7. Effect of natural convection on liquid formation (Ar = 0).

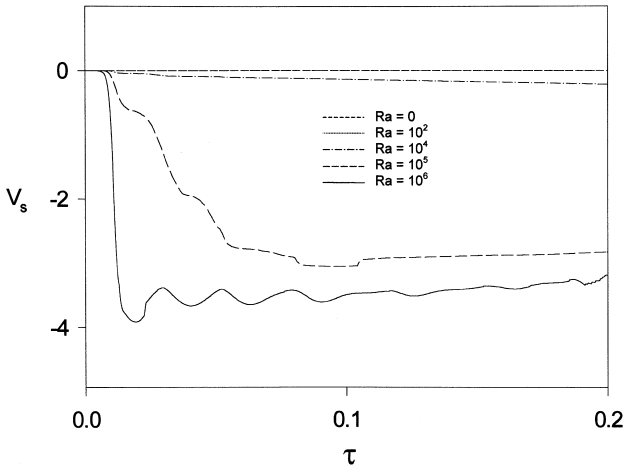

Fig. 8. Effect of natural convection on V_s (Ar = 0).

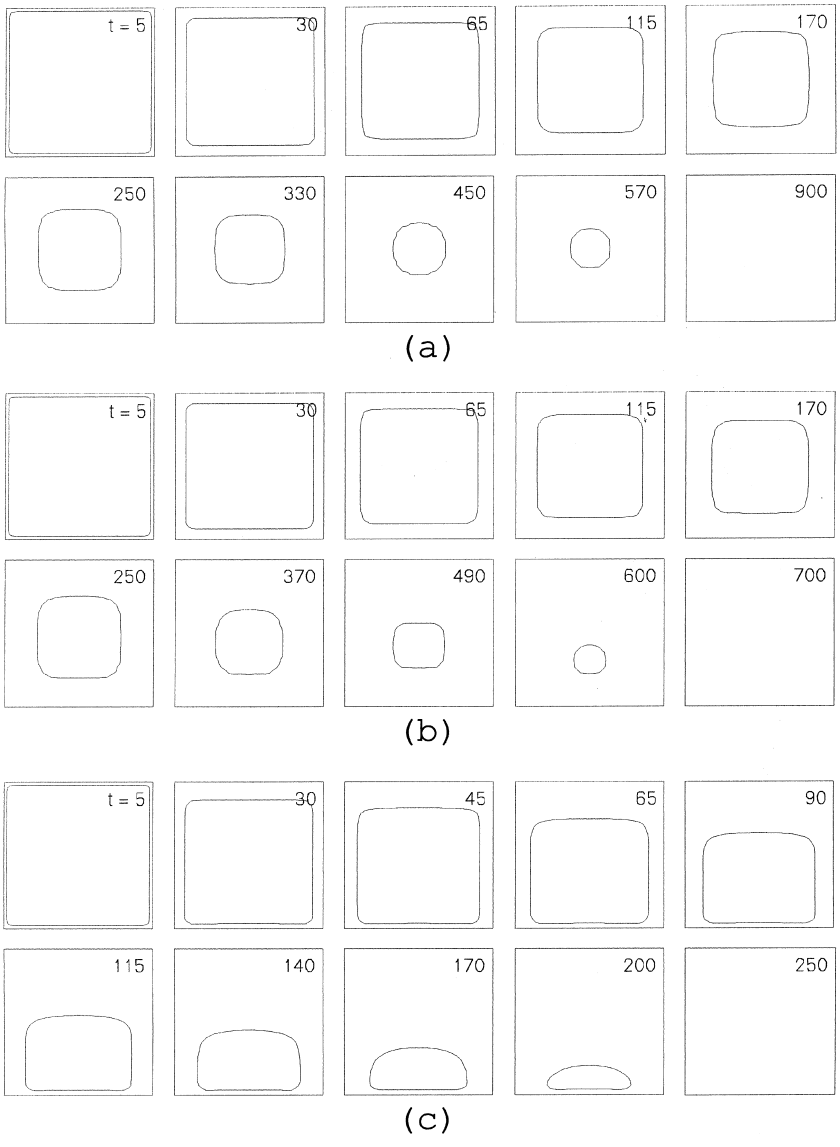

Fig. 9. Solid–liquid interface for Ar = 0 and (a) Ra = 0, (b) Ra = 10^4, and (c) Ra = 10^6. The numbers in the upper right corner indicate time ($\tau \times 10^3$).

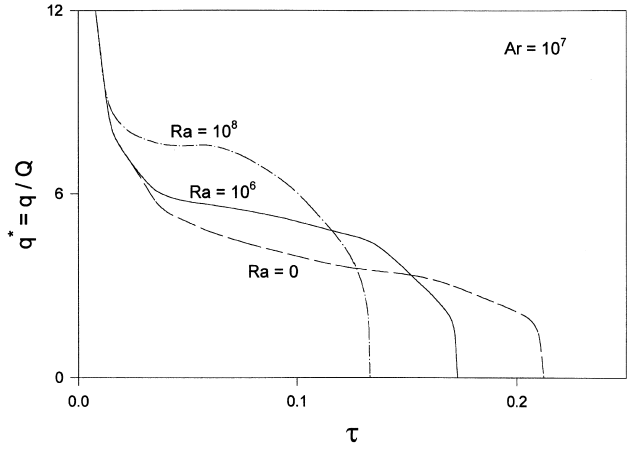

Fig. 10. Time variation of instantaneous rate of heat transfer at the solid–liquid interface.

zero, while the Ra varies from zero to 10^6. The remaining dimensionless parameters are kept constant at $Pr = 1$, $St = 0.1$, $\phi = 0$, and $A = 1$. Under these conditions, the percent of liquid formation with time is presented in Fig. 7. For $Ra = 0$, convection is absent and melting is only governed by conduction. As seen in the figure, the rate of liquid formation is increased with Ra. At higher values of Ra, the total melting is accomplished in a shorter time, since convection is also present in the melting process.

Velocity of the solid phase is presented in Fig. 8. For $Ra = 0$, the liquid is stagnant and the solid velocity is zero. As Ra is increased, the liquid moves due to the thermal buoyancy. As the solid is cold and the cavity walls are warm, the liquid exerts a downward shearing force on the lateral surface of the solid and causes it to move down. This solid motion, as evidenced from Fig. 8, is strengthened with Ra. It is noteworthy that $Ar = 0$, and the gravity does not directly cause the motion of the solid phase.

The solid–liquid interface for $Ra = 0$, 10^4 and 10^6, with other parameters kept constant as in Figs. 7 and 8, are shown in Fig. 9(a–c). The times corresponding to each diagram are also shown in the figure.

For $Ra = 0$ (Fig. 9(a)), conduction is the only mode of heat transfer, the solid remains in its original place, and the melting is symmetrical. As Ra is increased (Fig. 9(b) and c), melting is accompanied by the falling solid and the symmetry is clearly distorted. At $Ra = 10^6$, the falling motion has flattened the solid. In fact, the stronger natural convection and the impinging warm liquid has increased the melting rate at the top surface of the solid phase. Fig. 10 shows variation of the instantaneous rate of heat transfer at the solid–liquid interface with time. As Ra is increased, the natural convection begins to strengthen the melt motion induced by the direct falling of the solid phase. It is noteworthy that a nonzero Ar means that the solid phase is heavier than the surrounding liquid, and the descending motion of the solid brings about a forced convection liquid motion into effect.

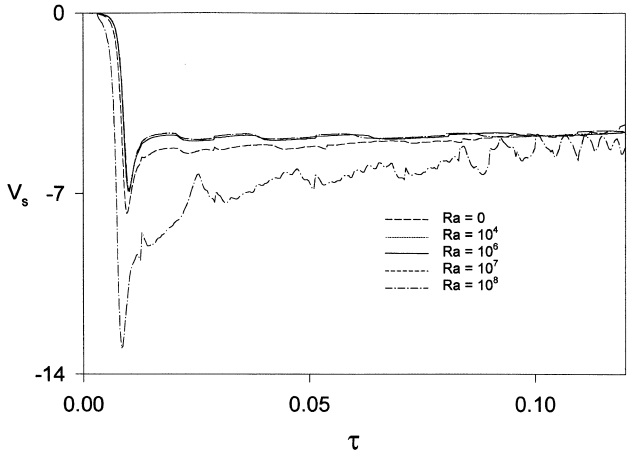

Fig. 11. Effect of natural convection on V_s ($Ar = 10^7$).

The velocity of the solid is plotted vs. time in Fig. 11. It is seen that even for $Ra = 0$ (absence of natural convection), the solid phase falls at a relatively high velocity due to gravity. This velocity is even higher than those shown in Fig. 8 for the largest value of Ra. As Ra is increased, the solid velocity increases further, since the recirculations caused by the resulting natural convection exert an additional downward shearing force on it. The noisy fluctuations seen in the curve for $Ra = 10^8$ are possibly due to approaching the threshold of liquid instability and transition.

5. Concluding remarks

A numerical investigation was carried out to study isothermal melting in a rectangular cavity using the fixed-grid enthalpy formulation. The solid phase was unfixed and could move during the melting process.

For $Ar = 0$ and $Ra = 0$, there was no liquid motion in the cavity and the melting progressed by conduction. As Ra was increased with $Ar = 0$, natural convection appeared in the liquid, which exerted a downward shearing force on the solid, and the solid was driven down.

The downward motion of the solid could also be generated by a nonzero Archimedes number. It was found that the liquid flow induced by a nonzero Ar is by far more active than that caused by natural convection. In this case, the melting progressed at a faster rate. The results indicated that, in general, the flow field is more active in the upper region of the cavity and more melting of the solid surface is observed there.

References

Asako, Y., Faghri, M., Charmchi, M., Bahrami, P.A., 1994. Numerical solution for melting of unfixed rectangular phase-change material under low-gravity environment. Numer. Heat Transfer, Part A 25, 191–208.

Ashgriz, N., Poo, J.Y., 1991. FLAIR: flux line segment model for advection and interface reconstruction. J. Comput. Phys. 93, 449.

Bareiss, M., Beer, H., 1984. An analytical solution of the heat transfer process during melting of unfixed solid phase change material inside a horizontal tube. Int. J. Heat and Mass Transfer 27, 739–746.

Beeckermann, C., Viskanta, R., 1989. Effect of solid subcooling on natural convection melting of pure metal. ASME J. Heat Transfer 11, 416–424.

Benon, W.D., Incropera, F.P., 1988. Developing laminar mixed convection with solidification in a vertical channel. ASME J. Heat Transfer 110, 410–415.

Brent, A.D., Voller, V.R., 1988. Enthalpy porosity technique for modeling convection–diffusion phase change. Numer. Heat Transfer 13, 297–318.

Cao, Y., Faghri, A., 1990. A numerical analysis of phase-change problems including natural convection. ASME J. Heat Transfer 112, 812–816.

Chang, W.J., Yang, D.F., 1996. Natural convection for the melting of ice in porous media in a rectangular enclosure. Int. J. Heat and Mass Transfer 39, 2333–2348.

Chi-Keung, C., Caldwell, J., 1996. Application of broyden's method to the enthalpy method for phase change problems. Numer. Heat Transfer, Part A 30, 575–587.

Crank, J., 1984. Free and Moving Boundary Problems. Clarendon Press, Oxford.

De Vahl Davis, G., 1983. Natural convection of air in a square cavity A benchmark numerical solution. Int. J. Numer. Meth. Fluids 3, 249–264.

Dong, Z.F., Chen, Z.Q., Wang, Q.J., 1991. Experimental and analytical study of contact melting in a rectangular cavity. J. Thermophysics 5, 347–353.

Gau, C., Viskanta, R., 1986. Melting and solidification of a pure metal on a vertical wall. J. Heat Transfer 108, 174–181.

Moallemi, M.K., Viskanta, R., 1986. Analysis of close-contact melting heat transfer. Int. J. Heat and Mass Transfer 29, 855–867.

Moallemi, M.K., Webb, B.W., Viskanta, R., 1986. An experimental and analytical study of close-contact melting. J. Heat Transfer 108, 894–899.

Patankar, S.V., 1980. Numerical Heat Transfer and Fluid Flow. Hemisphere, Washington, DC.

Prakash, C., Samonds, M., Singhal, A.K., 1987. A fixed grid numerical methodology for phase change problems involving a moving heat source. Int. J. Heat and Mass Transfer 30, 2690–2694.

Rady, M.A., Mohanty, A.K., 1996. Natural convection during melting and solidification of pure metals in a cavity. Numer. Heat Transfer, Part A 29, 49–63.

Roy, S.K., Sengupta, S., 1990. Gravity-assisted melting in a spherical enclosure: effect of natural convection. Int. J. Heat and Mass Transfer 33, 1135–1147.

Voller, V.R., Prakash, C., 1987. A fixed grid numerical modeling methodology for convection–diffusion mushy region phase change problems. Int. J. Heat and Mass Transfer 30, 1709–1719.

Yoo, H., Ro, S.T., 1988. Melting with solid–liquid density change and natural convection in a rectangular cavity. In: Proceedings of the First KSME–JSME Thermal and Fluid Engineering Conference vol. 1. pp. 100–105.

Zerrokal, M., Chatwin, C.R., 1994. Computational Moving Boundary Problems. Research Studies Press.